Article ID: 1000-324X(2023)06-0687-06 **DOI:** 10.15541/jim20220696

Enhanced Band-edge Luminescence of CuI Thin Film by Cl-doping

YANG Yingkang[1], SHAO Yiqing[1], LI Bailiang[1], LÜ Zhiwei[1], WANG Lulu[2], WANG Liangjun[1], CAO Xun[1,2], WU Yuning[1], HUANG Rong[1,3], YANG Chang[1]

(1. Key Laboratory of Polar Materials and Devices (Ministry of Education), School of Physics and Electronic Science, East China Normal University, Shanghai 200241, China; 2. Shanghai Institute of Ceramics, Chinese Academy of Sciences, Shanghai 200050, China; 3. Collaborative Innovation Center of Extreme Optics, Shanxi University, Taiyuan 030006, China)

Abstract: Wide band gap γ-CuI is a p-type transparent semiconductor with excellent optoelectronic and thermoelectric property, which has recently attracted worldwide attention. However, as an emerging material, its luminescence mechanism that is impacted by defects is rarely reported and remains obscure, limiting its further applications. In this work, Cl-doped CuI film was prepared by gas-phase reaction method. Using cathodoluminescence spectroscopy, effects of Cl doping on the surface morphology and cathodoluminescence property of CuI films were investigated in detail, and main defects of Cl presence in CuI films were explored by combining first-principle calculations, revealing relationship between structure and luminescent property of Cl-doped CuI films. These data showed Cl-doped region had a smoother surface than that of the undoped region with granular morphology, which clearly demonstrated that Cl dopant altered surface structure of the undoped region. Compared with the undoped region, the Cl dopant induced doubled fluorescence signal of band-edge emission at 410 nm, but reduced the defect peak at 720 nm, indicating that a small amount of Cl dopant brought a great luminescent improvement to CuI. The formation energy calculations of various crystal defects suggest that Cl can inhibit the formation of deep-level defects such as I vacancy in CuI and reduce the probability of non-radiative transition of excitons, which is consistent with the cathodoluminescence results. The full width at half maximum of the band-edge luminescence peak of Cl-doped CuI film is as small as 7 nm, showing extremely high luminescence monochromaticity. Therefore, the present findings deepen our understanding on how halogen doping boosts the luminescence performance of CuI-based materials.

Key words: CuI; Cl-doping; cathodoluminescence; first principle calculation

γ-CuI is a p-type transparent semiconductor material with a wide and direct bandgap of 3.05 eV at room temperature. Its high exciton binding energy (58 meV), high hole mobility (>40 $cm^2 \cdot V^{-1} \cdot s^{-1}$ in bulk)[1-2], large Seebeck coefficient and low thermal conductivity made it promising for optoelectronic and thermoelectric applications[1-8]. It has been integrated with other semiconductors such as GaN[9], ZnO[10], and β-Ga_2O_3[11] for fabrication of heterostructure devices. In addition, CuI is suitable for large-scale fabrication because of its low cost and mild synthesis conditions.

In recent years, excellent luminescence property of CuI have attracted wide interest. The PL peak of CuI film reported by Ahn, *et al.*[9] was one order of magnitude higher than that of commercial undoped GaN film at room temperature, and a hybrid n-GaN/p-CuI blue LED was developed. The luminescence of CuI at the room temperature is composed of the near-band-edge (NBE) emission and deep-level (DL) emission. The NBE emission consists of a sharp peak at 410 nm originated from the recombination of free excition and a broad band at 420–430 nm related to its intrinsic defects such as the copper vacancies and excess I[12]. The DL emission exhibits a broad band at 680–720 nm, which is originated from the I vacancies[13-14]. Yu, *et al.*[15] investigated the effect of growth temperature on luminescence perfor-

Received date: 2022-11-21; **Revised date:** 2022-12-26; **Published online:** 2023-02-13
Foundation item: National Key Research and Development Program of China (2017YFA0303403); Shanghai Science and Technology Innovation Action Plan (19JC1416700); National Natural Science Foundation of China (62074056, 61974042, 11774092)
Biography: YANG Yingkang (2002–), female, Bachelor. E-mail: 10192100516@stu.ecnu.edu.cn
杨颖康(2002–), 女, 学士. E-mail: 10192100516@stu.ecnu.edu.cn
Corresponding author: HUANG Rong, professor. E-mail: rhuang@ee.ecnu.edu.cn; YANG Chang, professor. E-mail: cyang@phy.ecnu.edu.cn
黄 荣, 教授. E-mail: rhuang@ee.ecnu.edu.cn; 杨 长, 研究员. E-mail: cyang@phy.ecnu.edu.cn

mance of sputtered CuI thin film, and optimized the optical performance at 300 ℃. Chen, *et al.*[16] reported efficient photoluminescence ink prepared using Cu-I cluster-based hybrid materials for biological imaging. However, it is still a challenge to promote the NBE emission (especially the band-edge emission) and meanwhile suppress the DL emission for potential applications.

Halogen doping is one of the most important strategy to tailor the luminescence of CuI. The Ⅰ-VII copper halides including CuCl, CuBr and CuI are all p-type wide bandgap semiconductors with high exciton binding energies of 190, 108, and 58 meV[17], respectively, which are believed to show excellent luminescence property. The luminance of polycrystalline CuCl films on Si substrate is 23 orders of magnitude higher than that of undoped single crystal GaN at room temperature[18]. When Cl or Br substitute I site in the CuI lattice, the difference in the p-orbital energy level of halogen elements can significantly affect the electronic structure and defect energy level position of CuI[19]. Li, *et al.*[13] found that Cl doping can enhance the NBE emission and suppress the DL emission of CuI effectively with an optimum concentration of 10% (in mol). However, most of researches focused on the photoluminescence of CuI single crystal and powder samples synthesized at relatively high temperature. In this work, Cl-doped CuI thin films were investigated in detail by scanning electron microscope (SEM) and cathodoluminescence spectroscope (CL). The band-edge emission at 410 nm and the DL emission within 680–720 nm from the areas with different doping levels were compared. The mechanism of the enhanced band-edge emission by Cl doping was revealed by the first principles calculations.

1 Experimental

1.1 Preparation of the film

The Cl-doped CuI film was prepared by gas-phase reaction method. The copper film was prepared by magnetron sputtering with Ar gas pressure of 2 Pa. A copper metal target and a quartz substrate were used for sputtering with a DC power of 30 W for 5 min. The thickness of obtained Cu thin film was about 70 nm. The obtained Cu film sample was placed together with 10 g iodine particles (purity of 99.9%) and trace CuCl solution (CuCl was dissolved in ethanol at 1% (in mass)) in a quartz glass bottle with a height of 5 cm and a diameter of 3 cm, which was sealed and kept at 80 ℃ on a hot plate for 20 min for iodization and Cl doping at the same time. The obtained Cl-doped CuI thin film exhibited a thickness of about 220 nm.

1.2 Characterization of the thin film

The morphology of Cl-doped CuI thin films was observed by a scanning electron microscope (Zeiss Gemini SEM450) equipped with an X-ray energy dispersive spectrometer (EDS: Oxford UltimMax EXTREME) for the chemical analyses and a CL spectrometer (Gatan Monarc Pro) for the CL analyses. The accelerating voltages were set at 2 kV for imaging and 5 kV for analyses. The grating 300 lines/mm and the resolution of 0.32 nm were used for the CL analyses at room temperature.

1.3 Computational methods

The first-principles calculations were performed using density functional theory (DFT)[20-21] as implemented in the Quantum-Espresso package[22]. The structural optimization was done using Perdew-Burke-Eznerhof (PBE)[23] exchange-correlation functional, and the defect properties including formation energies and transition levels were based on Hybrid HSE06[24] functional. The energy cutoff for the plane-wave basis was selected as 450 eV, and a 216-atom supercell was employed for defect calculations. For type of each defect, the defect is constructed in this supercell. For example, Cl_I is simulated by substituting one out of 108 I atoms by a Cl atom.

The formation enthalpy $\Delta H_f(\alpha,q)$ of a defect α in the charge state q using the supercell model can be calculated using[25-28]

$$\Delta H_f(\alpha,q) = E(\alpha,q) - E(\text{host}) + \sum n_i(E_i+\mu_i) + q(E_\text{F}+\varepsilon_\text{VBM}) + E_\text{corr} \quad (1)$$

where $E(\alpha,q)$ is the total energy of the supercell with a defect α and charge state q, and E(host) is the total energy of the host perfect crystal. n_i is the number of the atoms of element I removed from (n_i is negative) or added to (n_i is positive) the supercell when forming the defect. E_i is the energy per atom of element I in its stable elemental phase, and μ_i is the chemical potential of element I. E_corr, which comes from the Coulomb interaction among the repeating charged defects, was treated using scheme of Lany and Zunger[26]. The Fermi level E_F can vary from 0 to bandgap, and ε_VBM is the valence band maximum (VBM) of the host system.

2 Results and discussion

2.1 Surface morphology

Fig. 1(a) shows a typical low magnification surface morphology of Cl-doped CuI thin film. Many irregular

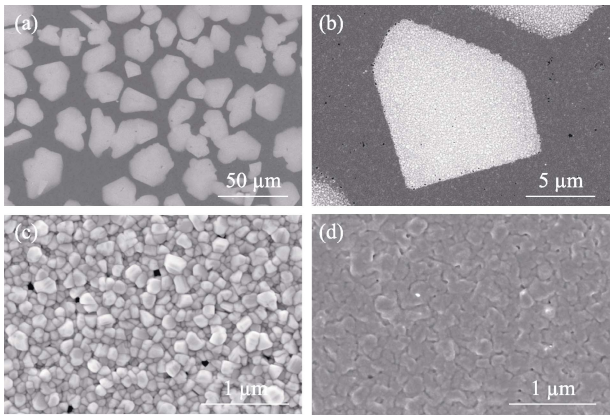

Fig. 1　Typical SEM images of the Cl-doped CuI thin film
(a) Low magnification; (b) High magnification; (c) High magnification image of the bright region; (d) High magnification image of the dark region

bright regions with the size of tens of micrometers can be seen in the dark background. The interface between the bright region and the dark region is very sharp and clear, as shown in Fig. 1(b). At high magnification (Fig. 1(c)), the bright regions exhibit the granular morphology with the grain size of ~100 nm, which is similar to the grain morphology of polycrystalline CuI films reported in the literature[1]. However, as shown in Fig. 1(d), the grains observed in the dark region are densely packed and connected, resulting in blurry grain boundaries and a relatively flat surface.

In order to know the difference between the regions with different contrast, EDS analyses were employed to obtain the chemical composition. Fig. 2(a) shows the SEM image of the EDS mapping area. Fig. 2(c) shows the corresponding Cu, I, Cl and Si elemental mappings. It can be seen that the contrast of Cu and I mappings are uniform. No obvious differences between the bright and dark regions can be discerned. However, relatively bright contrast can be seen in the dark regions of the Cl map. To confirm the Cl-rich in the dark region, two EDS spectra from the bright region (red) and the dark region (blue) were compared in Fig. 2(b) with the normalization of the Cu-L peak. An apparent Cl-K peak appears in the dark region. The quantifications of the EDS spectra reveal that the Cl concentration in the dark region is 2.69% (in mol) whereas the bright region keeps pure CuI. The lower anion/cation ratio in the dark region compared with the bright region indicates that the CuI sample is closer to the stoichiometry after Cl-doping.

In the synthesis of CuI thin film by gas-phase reaction, a small amount of Cl dopant reached the sample surface, occupying the I sites on the grain surface, and then diffused into the film. However, the distribution of Cl was not uniform due to the uncontrollable vapor flow. Also, the substrate temperature of ~80 ℃ was not high enough for sufficient Cl migration to reach the lowest free energy positions on the rough CuI surface, leading to surface phase segregations towards bright and dark regions. Such distinct two regions on the same sample were helpful for identifying the effects of Cl doping on CuI. Apparently, the Cl-doped dark region presented a more dense and flat morphology compared with the undoped bright region. Since Cl has a higher electron affinity than I and CuCl forms stronger bonding than CuI, it is likely that Cl can compensate the iodine-related defects on the CuI surface and thus improve the

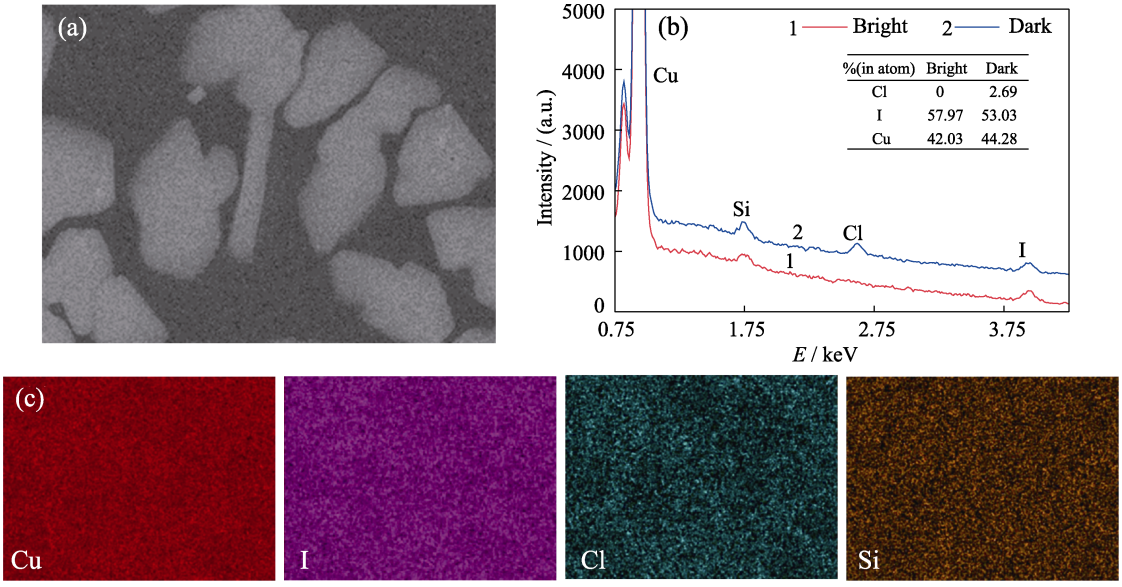

Fig. 2　EDS analyses of the Cl-doped CuI thin film
(a) SEM image of the mapping area; (b) Typical EDS spectra obtained from the bright region and the dark region; (c) EDS mappings of Cu, I, Cl and Si

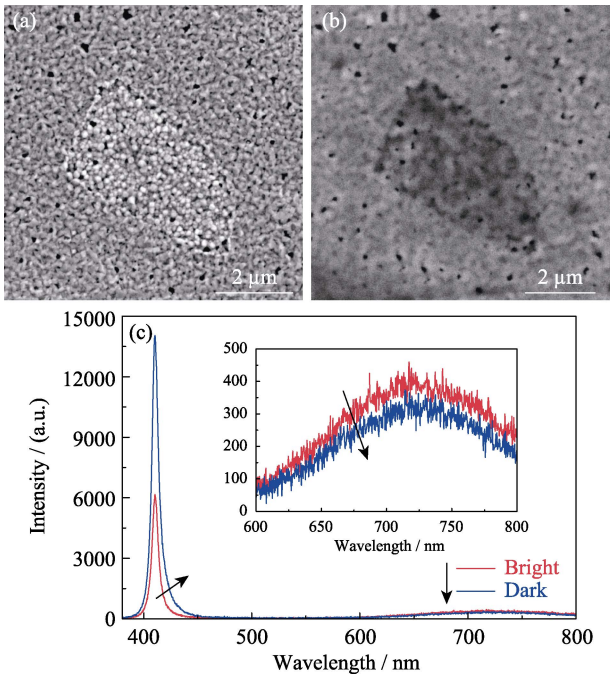

Fig. 3 CL analyses of the Cl-doped CuI thin film
(a) SEM image; (b) Panchromatic CL image; (c) Typical CL spectra acquired from the bright region and the dark region

surface morphology. At the same time, replacing I with Cl leads to fewer copper vacancy defects, which should be the reason of the lowered anion/cation ratio.

2.2 Luminescence property

Interestingly, the panchromatic CL images exhibited reversed contrast of SEM images, as shown in Fig. 3(a, b). The dark regions in the SEM image display brighter contrast in the CL image. It indicates that the emission intensity of the Cl-doped CuI regions is much stronger than the pure CuI regions. Fig. 3(c) shows typical CL spectra from the Cl-doped dark region (blue) and the bright pure CuI region (red) with exactly the same experimental conditions. A very sharp peak at 410 nm which originates from the band-edge emission and a broad DL emission at around 720 nm which might be caused by V_I-related defects are observed in both spectra. However, the intensity of the 410 nm peak from the Cl-doped CuI is ~2.5 times of that from the pure CuI. Furthermore, the intensity ratio of the peaks at 410 and 720 nm increases from 13.4 to 38.5 after Cl doping, suggesting greatly enhanced band-edge emission and suppressed DL emission.

In addition, the band-edge emission at 410 nm doesn't shift with the Cl-doping and no defects related NBE emission around 420 nm are detected in the present study, as shown in the inset of Fig. 3(c). It indicates negligible luminescence contributions from shallow energy level defects, which were abundant in the powder CuI samples synthesized at high temperature[14]. The full width at half maximum (FWHM) value of the band-edge emission peak is as small as 7 nm, better than many traditional LEDs[29-30], indicating an excellent monochromaticity of the Cl-doped CuI thin film. About 2.69% (in atom) Cl doping doubled the band-edge emission luminescence intensity of CuI, which might be related to the higher exciton binding energy of CuCl compared to CuI. The Cl dopant compensated the V_I-related defects and the iodization of Cu film at low temperature (80 ℃) eliminated the formation of the V_{Cu}-related defects, resulting in strongly suppressed non-radiative recombination, the defects related NBE emission and DL emission. Consequently, an enhanced band-edge luminescence was obtained in Cl-doped CuI thin films.

To further understand the effects of Cl doping on the crystal defects in CuI thin films, the formation energies of various defects including the Cl_I substitution were calculated with the conditions of Cu-rich and I-rich by the first principles calculations. The results are shown in Fig. 4. It can be seen that the defect Cl_I is not ionized and maintains neutral for the whole range of bandgap, indicating that Cl_I does not introduce defect energy levels into the band gap. On the other hand, the formation energy of Cl_I substitution defects is only 0.10 eV under Cu-rich conditions and 0.58 eV under I-rich conditions (purple lines in Fig. 4). They are lower than most of the intrinsic defects in CuI, especially the defects such as V_I that introduce deep levels into the band gap[31]. This means that the Cl dopant is easy to fill in I vacancy or replace I to form Cl_I, which effectively inhibits the generation of deep energy level defects such as V_I. It reduces the probability of non-radiative transitions in excitons in Cl-doped CuI regions, leading to stronger luminescence intensity than that of the undoped CuI regions.

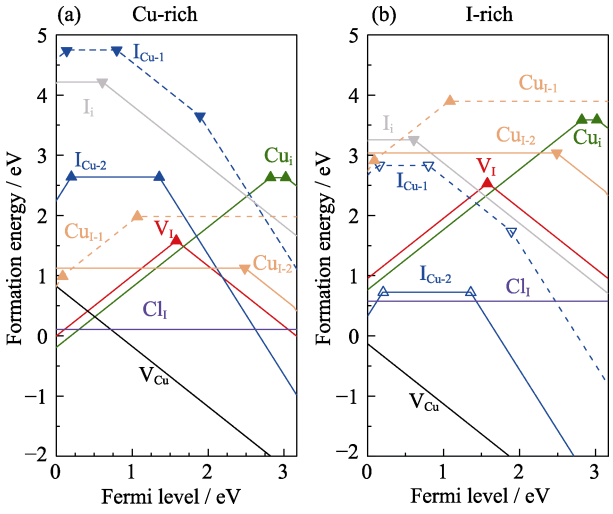

Fig. 4 Calculated formation energies of Cl_I and the most intrinsic defects in CuI as functions of the Fermi level
(a) Cu-rich condition; (b) I-rich condition

3 Conclusions

In summary, the Cl-doped CuI thin films made by the gas-phase reaction method consist of bright region (pure CuI) and dark region (Cl-doped CuI) in SEM image. The CL intensity of the 410 nm sharp peak originated from the band-edge emission in the Cl-doped region is more than two times of that in the undoped region, revealing greatly enhancement of the band-edge emission and effective suppression of the DL emission. The first principles calculations found that the Cl_I defect has a shallow forming energy. Thus, Cl doping might inhibit the defects in the V_I iso-deep energy level effectively, thereby reducing the probability of non-radiative transitions in excitons. Our findings pave the way for the future development of high-performance CuI-based optoelectronic devices such as LEDs and scintillators by halogen doping.

References:

[1] GRUNDMANN M, SCHEIN F L, LORENZ M, *et al.* Cuprous iodidea p-type transparent semiconductor: history and novel applications. *Physica Status Solidi (a)*, 2013, **210(9):** 1671.

[2] YANG C, KNEIB M, LORENZ M, *et al.* Room-temperature synthesized copper iodide thin film as degenerate p-type transparent conductor with a boosted figure of merit. *Proceedings of the National Academy of Sciences*, 2016, **113(46):** 12929.

[3] YANG Z, WANG M, SHUKLA S, *et al.* Developing seedless growth of ZnO micro/nanowire arrays towards ZnO/FeS_2/CuI P-I-N photodiode application. *Scientific Reports*, 2015, **5(1):** 11377.

[4] ZHOU Z, LI X, ZHAO F, *et al.* Self-powered heterojunction photodetector based on thermal evaporated p-CuI and hydrothermal synthesised n-TiO_2 nanorods. *Optical Materials Express*, 2022, **12(2):** 392.

[5] NIU S, ZHAO F, HANG Y, *et al.* Enhanced p-CuI/n-ZnO photodetector based on thermal evaporated CuI and pulsed laser deposited ZnO nanowires. *Optics Letters*, 2020, **45(2):** 559.

[6] LESCOP C. Coordination-driven supramolecular synthesis based on bimetallic Cu(I) precursors: adaptive behavior and luminescence. *The Chemical Record*, 2020, **21(3):** 544.

[7] INAGAKI S, NAKAMURA M, OKAMURA Y, *et al*. Heteroepitaxial growth of wide bandgap cuprous iodide films exhibiting clear free-exciton emission. *Applied Physics Letters*, 2021, **118(1):** 012103.

[8] YANG C, SOUCHAY D, KNEISS M, *et al.* Transparent flexible thermoelectric material based on non-toxic earth-abundant p-type copper iodide thin film. *Nature Communications*, 2017, **8:** 16076.

[9] AHN D, SONG J D, KANG S S, *et al.* Intrinsically p-type cuprous iodide semiconductor for hybrid light-emitting diodes. *Scientific Reports*, 2020, **10(1):** 3995.

[10] YANG C, KNEIß M, SCHEIN F L, *et al.* Room-temperature domain-epitaxy of copper iodide thin films for transparent CuI/ZnO heterojunctions with high rectification ratios larger than 10^9. *Scientific Reports*, 2016, **6(1):** 21937.

[11] VENKATA KRISHNA RAO R, RANADE A K, DESAI P, *et al.* Temperature-dependent device properties of γ-CuI and β-Ga_2O_3 heterojunctions. *SN Applied Sciences*, 2021, **3(10):** 796.

[12] PERERA V P S, TENNAKONE K. Recombination processes in dye-sensitized solid-state solar cells with CuI as the hole collector. *Solar Energy Materials and Solar Cells*, 2003, **79(2):** 249.

[13] LI F, GU M, LIU X, *et al.* Enhancement of the near-band-edge emission of CuI by Cl doping. *Journal of Luminescence*, 2019, **205:** 337.

[14] GAO P, GU M, LIU X, *et al.* Crystal growth and luminescence properties of CuI single crystals. *Optik*, 2014, **125(3):** 1007.

[15] YU W, BENNDORF G, JIANG Y, *et al.* Control of optical absorption and emission of sputtered copper iodide thin films. *Physica Status Solidi (RRL) - Rapid Research Letters*, 2020, **15(1):** 2000431.

[16] CHEN C, LI R H, ZHU B S, *et al.* Highly luminescent inks: aggregation-induced emission of copper-iodine hybrid clusters. *Angewandte Chemie International Edition*, 2018, **57(24):** 7106.

[17] AHN D, PARK S H. Cuprous halides semiconductors as a new means for highly efficient light-emitting diodes. *Scientific Reports*, 2016, **6:** 20718.

[18] COWLEY A, FOY B, DANILIEUK D, *et al.* UV emission on a Si substrate: optical and structural properties of γ-CuCl on Si grown using liquid phase epitaxy techniques. *Physica Status Solidi (a)*, 2009, **206:** 923.

[19] FERHAT M, ZAOUI A, CERTIER M, *et al.* Electronic structure of the copper halides CuCl, CuBr and CuI. *Materials Science and Engineering B*, 1996, **39:** 95.

[20] HOHENBERG P, KOHN W. Inhomogeneous electron gas. *Physical Review*, 1964, **136(3B):** B864.

[21] KOHN W, SHAM L J. Self-consistent equations including exchange and correlation effects. *Physical Review*, 1965, **140(4A):** A1133.

[22] GIANNOZZI P, BARONI S, BONINI N, *et al.* QUANTUM ESPRESSO: a modular and open-source software project for quantum simulations of materials. *J. Phys.: Condens. Matter*, 2009, **21(39):** 395502.

[23] PERDEW J P, BURKE K, ERNZERHOF M. Generalized gradient approximation made simple. *Physical Review Letters*, 1996, **77(18):** 3865.

[24] HEYD J, SCUSERIA G E, ERNZERHOF M. Hybrid functionals based on a screened Coulomb potential. *The Journal of Chemical Physics*, 2003, **118(18):** 8207.

[25] MAKOV G, SHAH R, PAYNE M C. Periodic boundary conditions in *ab initio* calculations. II. Brillouin-zone sampling for aperiodic systems. *Physical Review B*, 1996, **53(23):** 15513.

[26] LANY S, ZUNGER A. Assessment of correction methods for the band-gap problem and for finite-size effects in supercell defect calculations: case studies for ZnO and GaAs. *Physical Review B*, 2008, **78(23):** 235104.

[27] FREYSOLDT C, GRABOWSKI B, HICKEL T, *et al.* First-principles calculations for point defects in solids. *Reviews of Modern Physics*, 2014, **86(1):** 253.

[28] CHEN H, WANG C Y, WANG J T, *et al.* First-principles study of point defects in solar cell semiconductor $CuInS_2$. *Journal of Applied Physics*, 2012, **112(8):** 084513.

[29] CHOI J H, ZOULKARNEEV A, KIM S I, *et al.* Nearly single-crystalline GaN light-emitting diodes on amorphous glass substrates. *Nature Photonics*, 2011, **5(12):** 763.

[30] KRIEG L, MEIERHOFER F, GORNY S, *et al.* Toward three-dimensional hybrid inorganic/organic optoelectronics based on GaN/oCVD-PEDOT structures. *Nature Communications*, 2020, **11(1):** 5092.

[31] LIU D, CAI Z, WU Y N, *et al.* First-principles identification of V_I+Cu_i defect cluster in cuprous iodide: origin of red light photoluminescence. *Nanotechnology*, 2022, **33(19):** 195203.

Cl 掺杂对 CuI 薄膜发光性能增强研究

杨颖康[1], 邵怡晴[1], 李柏良[1], 吕志伟[1], 王路路[2], 王亮君[1],
曹 逊[1,2], 吴宇宁[1], 黄 荣[1,3], 杨 长[1]

(1. 华东师范大学 物理与电子科学学院, 极化材料与器件教育部重点实验室, 上海 200241; 2. 中国科学院 上海硅酸盐研究所, 上海 200050; 3. 山西大学 极端光学协同创新中心,太原 030006)

摘 要: 宽禁带 γ-CuI 是一种具有优异光电和热电性能的 p 型透明半导体材料, 近年来受到广泛关注。但作为一种新兴材料, 其发光性能受材料缺陷影响的物理机理尚不清楚。本工作通过气相反应法制备了 Cl 掺杂的 CuI 薄膜, 采用电镜表征方法研究 Cl 掺杂对多晶 CuI 薄膜表面形貌和阴极荧光发光特性的影响, 并结合第一性原理计算探究了 Cl 在 CuI 薄膜中的主要存在形式, 以揭示 Cl 掺杂 CuI 薄膜结构与发光性能的联系。研究结果表明, 原本晶粒饱满但晶界显著的 CuI 薄膜掺杂 Cl 后呈现出致密平整的表面, 表明 Cl 掺杂剂改变了 CuI 的表面结构。相比未掺杂区域, Cl 掺杂区 410 nm 处的荧光信号明显得到双倍增强, 而在 720 nm 附近的缺陷峰则略有降低, 说明 Cl 掺杂极大改善了 CuI 薄膜的发光性能。通过第一性原理计算对该现象进行理论分析, 发现引入 Cl 元素有效抑制了 CuI 中碘空位等深能级缺陷的产生, 降低了激子发生非辐射跃迁的概率, 从而改善 CuI 的发光性能, 这与阴极荧光的结果一致。本研究获得的掺杂 CuI 薄膜带边发光峰的半峰宽仅为 7 nm, 表现出极高的发光单色性。这些发现有助于对卤素掺杂获得的高性能 CuI 基材料的理解。

关 键 词: CuI; Cl 掺杂; 阴极荧光; 第一性原理计算

中图分类号: TQ174 **文献标志码:** A